Chapter

Nanomaterials Characterisation through Magnetic Field Dependent AFM

Marco Coïsson, Gabriele Barrera, Federica Celegato and Paola Tiberto

Abstract

Atomic force microscopy is a versatile technique allowing to exploit many different physical effects for measuring a number of materials properties. The magnetic properties of surfaces and thin films are traditionally accessed through magnetic force microscopy, which produces magnetic field gradient maps generated by the magnetisation distribution at the surface of the sample. However, more advanced techniques can be derived from this fundamental setup, allowing for a richer characterisation of magnetic samples. In this chapter, we will describe how to extend a magnetic force microscope to allow magnetic field-dependent characterisations. Magnetisation reversal processes, as well as full hysteresis loops, can be investigated with such a technique, with field resolution adequate for identifying significant features such as domains reversal, nucleation or annihilation of domains, and other irreversible mechanisms. The same principle can also be exploited for the measurement of magnetostriction on thin films, and can be taken as guideline for other advanced applications of atomic force microscopy.

Keywords: MFM, magnetostriction, hysteresis loops, thin films

1. Introduction

Magnetic force microscopy [1] is a technique developed more than thirty years ago that is derived from atomic force microscopy [2]. It exploits an AFM tip that is coated with a magnetic material, and therefore acquires a magnetic moment. The tip becomes sensitive to the magnetic force gradient acting between the surface of a magnetic sample and the tip itself [3, 4], and allows the microscope to build local magnetisation maps at scales well below the micrometer [5].

In the course of the years, MFM has proven to be an extremely powerful technique to study a variety of magnetic systems, including patterned media [6, 7], cellular automata [8], individual magnetic nanostructures [9], or phase separations in magnetic materials at the nanoscale [10]. While its most straightforward application is the imaging of magnetic domains configurations at the sample magnetic remanence, several attempts have been made to adapt MFM to the study of the magnetisation reversal processes induced by an applied magnetic field [11–15]. These approaches opened new ways of exploiting the powerful MFM technique to the study of time-evolving magnetic domains configurations, whose changes are

triggered by variations in an applied magnetic field, letting MFM characterisations expand toward the typical domain of magneto-optic microscopy, although with a much higher space resolution [16] but also with much slower time scales.

In this chapter, we will summarise a magnetic field-dependent MFM approach that is based on the single-point technique [5]. We will show how this advanced AFM application can be exploited to investigate magnetic field-induced magnetisation reversal processes at the nanoscale on different sets of magnetic materials, and we will show that the basic principles of this technique are sufficiently general to allow many different experiment designs for the study e.g. of hysteresis loops, local magnetic anisotropies, magnetostriction.

2. Magnetic field-dependent MFM

Magnetic force microscopy is an application derived from atomic force microscopy, that belongs to the family of the so-called "2nd pass" techniques. Their name derives from the fact that the microscope scans each line two times (usually back and forth each time): in the first scan, or pass 1, the AFM operates in intermittent contact mode and acquires the morphology of the sample along the scanned profile; in the second scan, or pass 2, the AFM operates in "lift mode", i.e. the cantilever is kept in oscillation but in non-contact mode, by lifting the scan height at a certain constant level above the sample surface (usually a few tens of nanometers). In this way, the short-range interactions typical of the Lennard-Jones-type potential become negligible, and long-range interactions such as the elctrostatic or magnetostatic ones can be investigated, provided that the microscope tip is coated by a suitable material. In the case of the MFM technique, the tip must be coated with a magnetic material, whose magnetisation must also lie along a known (and constant) direction (usually along the tip axis, perpendicular to the sample plane). When interacting with the sample surface, in pass 2, the MFM tip senses the second derivative of the z (vertical) component of the magnetic fields fringing from the sample surface, with respect to the z direction (i.e. $\partial^2 H_z/\partial z^2$), and as a result the cantilever oscillation amplitude, phase and frequency are affected. Typically, either the cantilever oscillation frequency or its phase are taken as signals for representing the magnetostatic interaction with the sample. In the following, all MFM images that will be shown will use the phase signal.

As this interaction happens through $\partial^2 H_z/\partial z^2$, it is necessary that fringing fields with a H_z component emerge from the surface of the sample in proximity of the tip position. This is typically possible in a few different cases, such as:

- a domain wall (either Bloch or Néel) is located underneath the tip, with the rest of the magnetisation lying in the sample plane;
- the sample is characterised by a perpendicular anisotropy;
- the sample is characterised by an in-plane magnetic anisotropy, but it is patterned in such a way that the magnetisation vector is not parallel to some of the patterns sides.

In general, therefore, a MFM detects a magnetic domains configuration when surface magnetic charges or poles appear under the tip, either because the magnetisation is tilted off the sample plane, or because geometrical constraints force the magnetisation to develop free poles along some directions (e.g. obtained by lithography or patterning).

Normally, such a MFM is limited to the investigation of the magnetic domains configuration of samples at their magnetic remanence. Whatever their remanent state, this must have been obtained by submitting the sample to a magnetic field history by exploiting some other technique, and cannot be modified during the MFM investigations.

These constraints can be at least partly lifted if the microscope is equipped with a means of generating a magnetic field (i.e. an electromagnet or a coil), either in the sample plane, or perpendicular to it. The microscope should be adequately designed for this application, as it must not contain magnetic elements in the head and in the scanner, which could be damaged by the application of an external magnetic field, and which would probably induce unacceptable drifts in the operation of the microscope or artefacts in the acquisition of the images. With the possibility to apply a magnetic field during image acquisitions, the MFM becomes a tool for characterising samples not only at their magnetic remanence, but also at specific field values which are of interest to the experimenter.

An example of such an application is given in **Figure 1**, where square dots of $Fe_{50}Pd_{50}$ with a lateral size of 800 nm and a thickness of 35 nm have been

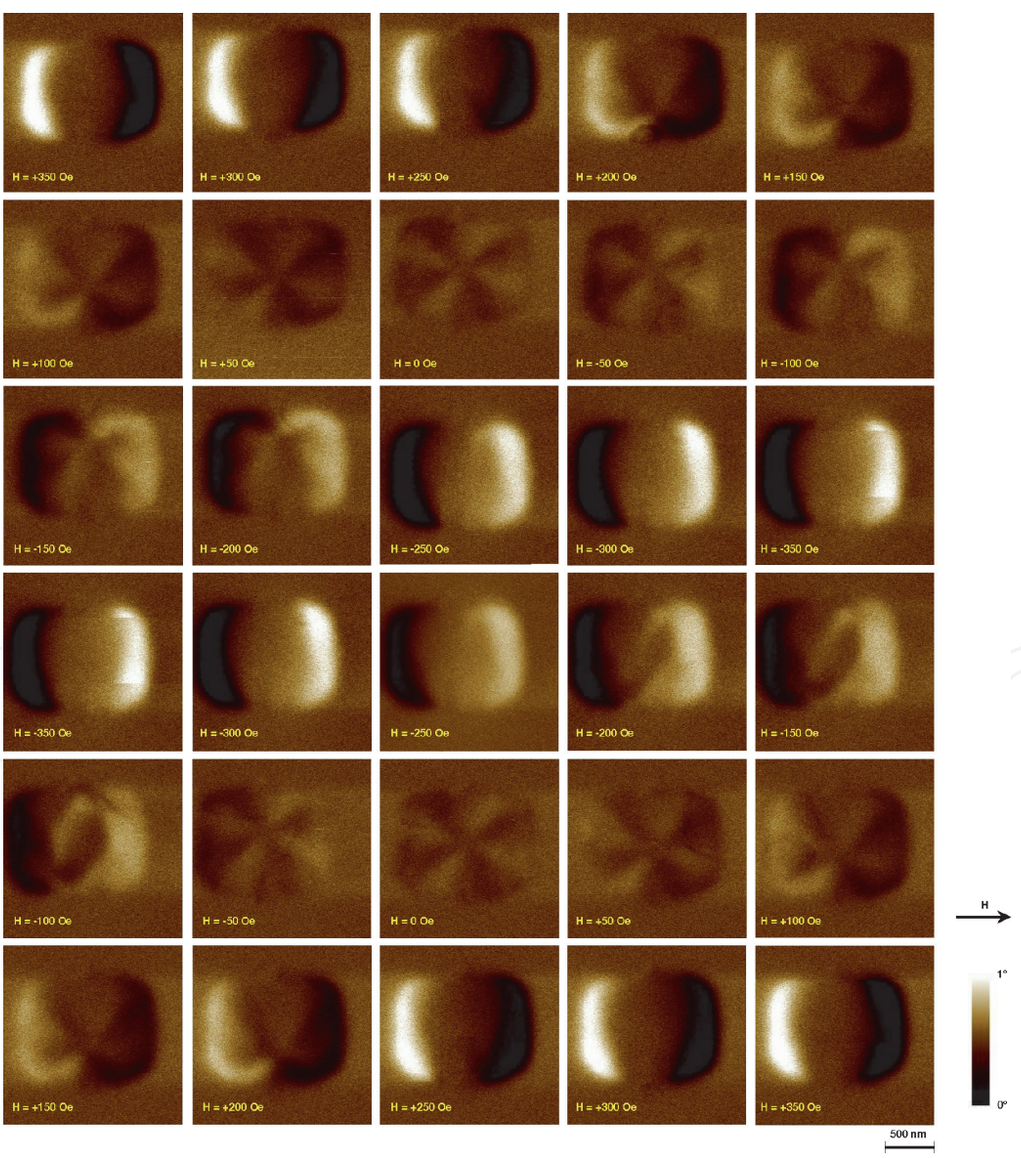

Figure 1.
MFM images (pass 2, phase channel) as a function of the applied magnetic field of $Fe_{50}Pd_{50}$ squares (lateral size 800 nm, thickness 35 nm). The images follow a whole hysteresis loop within the limits of ±350 Oe, at steps of 50 Oe. The magnetic field is applied along the horizontal direction. The tip used was a Bruker MESP-HR.

investigated as a function of the applied magnetic field. The field has been cycled from +350 Oe to -350 Oe and back, at steps of 50, to complete a hysteresis loop. The MFM images of **Figure 1** show how the domain configuration of one of such squares evolves with the field, from a saturated state (bright and dark contrast at opposite sides of the square), to the nucleation of a vortex, the motion of its centre along the direction perpendicular to the applied field, its annihilation, and finally to the opposite saturated state (reversed bright and dark contrast), and then back, with the occasional development of a more complex domain structure (see the images at -200, -150 and -100 Oe when going from negative to positive saturation).

While powerful, this approach is limited to only a few images at different applied fields, because of time constraints or magnetic tip wear-out.

3. A "dynamic scanning mode" MFM

The magnetic field-dependent MFM technique discussed in Section 2 presents the undoubted advantage that the magnetic domain configuration of the studied sample can be obtained with as much detail as desired for any applied magnetic field value. In this way, even complex magnetic structures can be studied along their evolution with the magnetic field, in a way similar to what magneto-optics systems offer, but with a much improved space resolution, typical of AFM-based techniques. However, this advantage holds for a big part only in principle. In fact, it is difficult if not impossible to acquire the large number of MFM images required to study magnetisation processes with high magnetic field resolution. A first constraint comes from the time required to acquire each image, which is often of several minutes or even a few tens of minutes, that makes the capture of hundreds or even thousands of images impractical. A second constraint is due to the fact that even a well-tuned AFM in intermittent-contact mode (as is normally operated an AFM when performing magnetic characterisations) slightly wears out the tip in the course of time. Normally, only a few tens of images can be obtained with a single tip, even by optimally operating the microscope, before artefacts start to appear and the tip performance degrades (including the magnetic performance, due to the progressive damage or detachment of the magnetic coating). While replacing the tip is technically feasible, scanning exactly the same field of view after the tip replacement may not be easy for certain samples, and the obtained image quality would probably depend on the tip, as its shape, sharpness, and magnetic coating characteristics fluctuate among specimens even of the same batch. Therefore, while in principle a thorough field-dependent investigation of a magnetic sample is feasible with a conventional MFM, it is often impractical or even impossible due to the constraints discussed above.

To overcome these limitations, a different approach has been exploited [5, 17, 18], consisting in condensing the information on the magnetisation processes as a function of a sufficiently resolved magnetic field in just a single image. The difference between a MFM operating in "normal scanning mode" (a conventionally operating MFM) and one operating in "dynamic scanning mode" is schematically represented in **Figure 2**.

A MFM in "normal scanning mode" works by scanning a portion of the sample by moving the tip relative to the sample along a direction conventionally called x (the fast scan axis), that reproduces a scan line. Then, the scan line is moved by a certain step along the direction conventionally called y (the slow scan axis), so that at the end of a frame the whole field of view (the magenta area in **Figure 2**) is covered. Each scanned line (there can be several hundreds or thousands, in **Figure 2** they are 400) explores a different profile of the sample, and all scan lines together

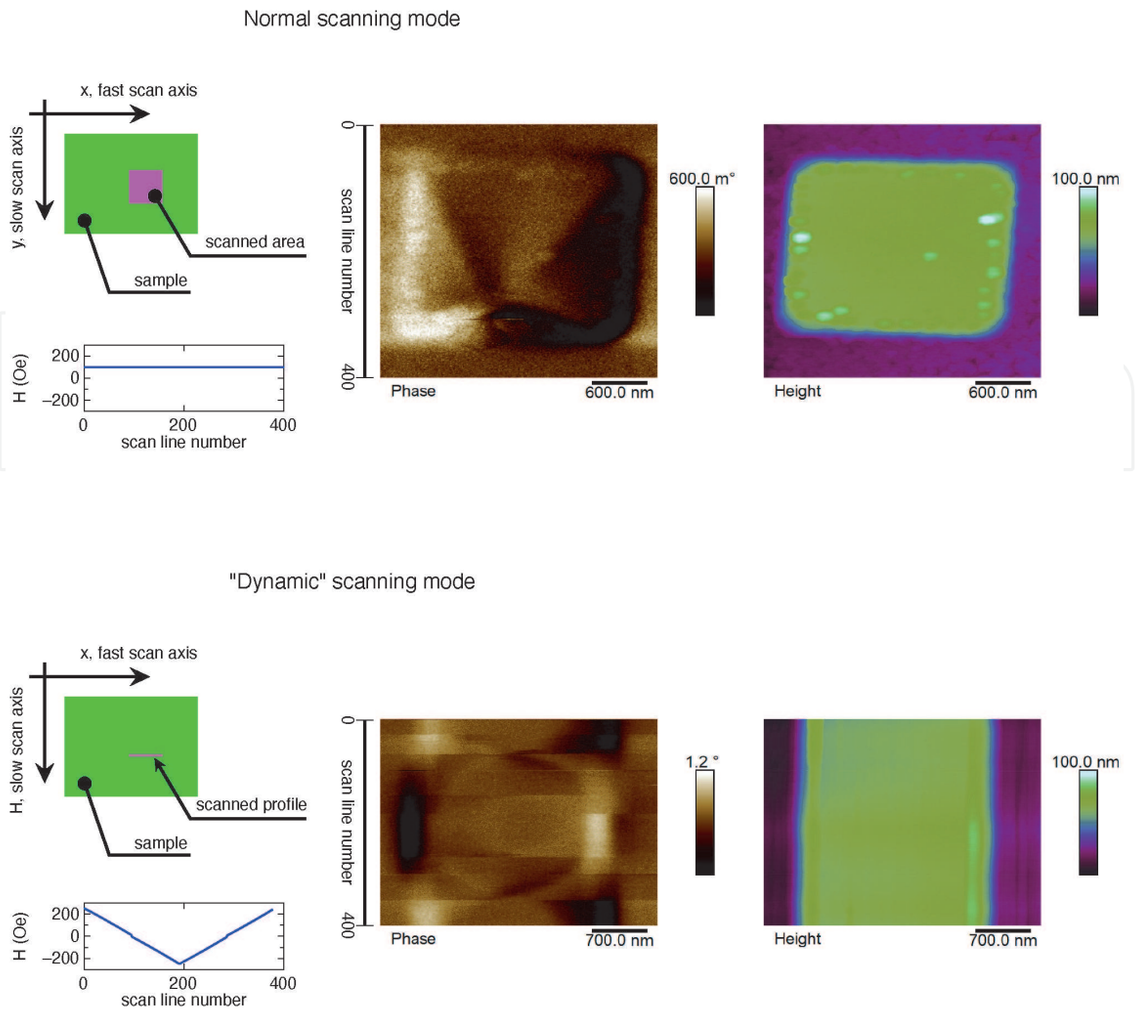

Figure 2.
Operation principle of an MFM in "normal" (upper panel) and "dynamic" (lower panel) scanning modes. Green rectangle: sample. Magenta square or line: area or line scanned by the MFM. The x position of the scan moves along the horizontal (fast) scan axis. In normal scanning mode: the y position of the scan moves along the vertical (slow) scan axis, while the applied magnetic field H is kept constant across each scanned line. In dynamic scanning mode: the y position of the scan does not move (slow scan axis disabled), whereas the applied magnetic field H changes at each scanned line. The right panels report typical MFM (phase channel, pass 2) and AFM (height channel, pass 1) images acquired in the two scanning modes for a $Fe_{50}Pd_{50}$ square dot (side 2 μm, thickness 35 nm) for a constant H = 100 Oe (normal mode) and for H cycling between ±250 Oe (dynamic mode). The tip was a Bruker MESP-HR.

make an image representing a certain surface area of the sample: for example, in the case of **Figure 2** in "normal scanning mode", a full AFM image of the investigated dot is obtained. In this operation mode, each scan line is acquired at the same applied magnetic field, e.g. 100 Oe in **Figure 2**. This is the way all MFM images of **Figure 1** have been captured.

A MFM in "dynamic scanning mode" works by disabling the slow scan axis. In this way, the field of view of the microscope is no longer a surface area, but just a single profile (**Figure 2**, bottom panel), since once the profile acquisition along the fast scan axis is complete the slow scan axis is not moved. However, as in the "normal scanning mode", the MFM image still consists of several hundreds or thousands of lines, although all along the same profile. If the geometrical *y* direction is removed from the image coordinates (as *y* remains constant), it is possible to assign the scan line number to a different input quantity that can be varied during the operation of the microscope. This input quantity could be e.g. the applied magnetic field. If the magnetic field is kept constant *during* the scan along the fast axis and is incremented *within* one profile scan and the next, then an image is

acquired (see **Figure 2** bottom panel) that for each line reproduces the *same* profile but under different conditions, i.e. under different magnetic fields: for the same dot studied above, the corresponding AFM image is then just a repetition of the same morphology for each line, the whole dot image is no longer reproduced as the scanning is never moved along the y (slow scan) axis (see **Figure 2**). In this way, a *single* MFM image contains in itself the information on how the magnetic configuration evolves under hundreds or even thousands of different applied field values. The drawback is that this information is limited to a 1-D profile, and not to a 2-D surface area as in "normal scanning mode" MFM.

A "dynamic scanning mode" MFM requires a few additional hardware than a conventional MFM. Above all, its controller must give access to a way to know when the microscope has finished acquiring a line. Depending on how this information is obtained, a suitable hardware and/or software combination must be developed to ensure that the applied magnetic field variations are properly synchronised with the scan line change. For example [17, 18], a TTL level could be output by the AFM controller signalling each EOL, and used to trigger the magnetic field step through a suitably programmed current generator or ramp generator. If the AFM controller provides external input channels, the voltage reading e.g. of a gaussmeter could be fed to the controller, therefore directly linking each scanned line with the corresponding magnetic field value. In this way, the obtained 2-D image contains along the x (fast scan) direction the usual spatial dependence, and along the y (slow scan) direction a line-number dependence that is implicitly defined through the channel acquiring the external (gaussmeter) input. The image then visually represents the magnetic field dependence of the domains configuration along a single profile.

This operation mode is sometimes called "dynamic", as opposed to the "normal" or "static" operation mode of MFM systems. In "normal scanning mode", the MFM acquires a single image under a static (constant) applied field, whereas in "dynamic scanning mode" the applied field varies with time (although it is constant during the acquisition of each line). The term "dynamic", therefore, does not imply that a frequency-dependent characterisation is performed, and, in this context, should be used consciously.

A representative application of the "dynamic" operation mode is the measurement of local hysteresis loops of magnetic patterned micro- and nano-structures [17]. An example of a typical measurement is shown in **Figure 3** for a $Fe_{50}Pd_{50}$ patterned square, with a lateral size of 800 nm and a thickness of 35 nm (the same sample whose domains configurations were shown in **Figure 1** for selected applied field values). **Figure 3(a)** shows the height channel: the MFM tip scans along a

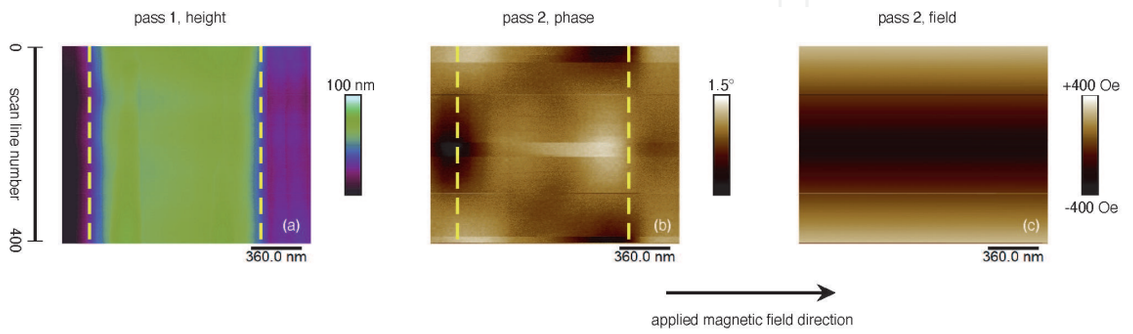

Figure 3.
Example of data acquisition in "dynamic scanning mode" for the measurement of a local hysteresis loop on a $Fe_{50}Pd_{50}$ square (lateral size 800 nm, thickness 35 nm). (a) Height channel (pass 1). The yellow dashed lines approximately mark the two lateral square edges. (b) Phase channel (pass 2), i.e. the magnetic response. The yellow dashed lines are placed in correspondence of those in panel (a). (c) AFM controller auxiliary input channel, set to receive the applied field value. The tip was a Bruker MESP-HR.

profile passing across the whole width of the FePd square. Since the microscope works in "dynamic" mode, the slow scan axis is disabled, and the same profile is repeatedly acquired. For this reason, the topography image in **Figure 3(a)** does not show significant variations for the different scan line numbers, as, ideally, exactly the same profile and therefore the same morphology are encountered during the scan of each line. Small fluctuations in the sample position, due e.g. to scanner drifts, are acceptable as long as the magnetic configuration under the tip is repeatable. The two dashed yellow lines in **Figure 3** approximately identify the position of the two side edges of the square, and are repeated in the same position in **Figure 3(b)**, where the phase channel in pass 2 is instead reported. This channel contains the magnetic response of the tip at the chosen lift scan height, and is therefore the channel to consider when looking at the magnetic domain configuration of the sample. **Figure 3(c)** reports the image acquired in pass 2 for the AFM controller auxiliary input, that, as described earlier, is fed with the gaussmeter reading. This channel, therefore, contains the applied field value for each scan line.

In order to build a local hysteresis loop from the acquired data, vertical sections must be extracted from the data reported in **Figure 3**, as described in **Figure 4**. From the magnetic response channel (**Figure 3(b)**), the phase values along the two dashed yellow lines are taken and their difference Δ_{phase} is calculated, as a function of the scan line number (**Figure 4(a)**). These data represent how the phase contrast evolves at the left and right sides of the $Fe_{50}Pd_{50}$ square as a function of the scan line number. Similarly, any vertical section of **Figure 3(c)** represents the evolution of the applied magnetic field with the scan line number, as shown in **Figure 4(b)**. Δ_{phase} and the applied field are both available as a function of a common parameter, i.e. the scan line number. If this parameter is taken out and the two quantities are plotted one against the other, the local hysteresis loop displayed in **Figure 4(c)** is obtained.

Local hysteresis loops obtained with this technique are not meant to be interpreted as the magnetic hysteresis loops measured e.g. with magnetometers, whose vertical axis is a magnetic moment or a magnetisation. Local hysteresis loops as those shown in **Figure 4(c)** do not plot a magnetisation as a function of the applied magnetic field, but a quantity that describes how the magnetisation is arranged in a specific portion of the sample, as a function of the applied magnetic field. In the case of the $Fe_{50}Pd_{50}$ square used in this example, the magnetic contrast at the left and right sides of the squares evolves with the applied field between "bright" and "dark" extrema, corresponding to the cases of uniform (saturated) magnetisation along the applied field direction (see **Figure 1**). All intermediate colour shades correspond to lower magnetic signals detected by the MFM tip in pass

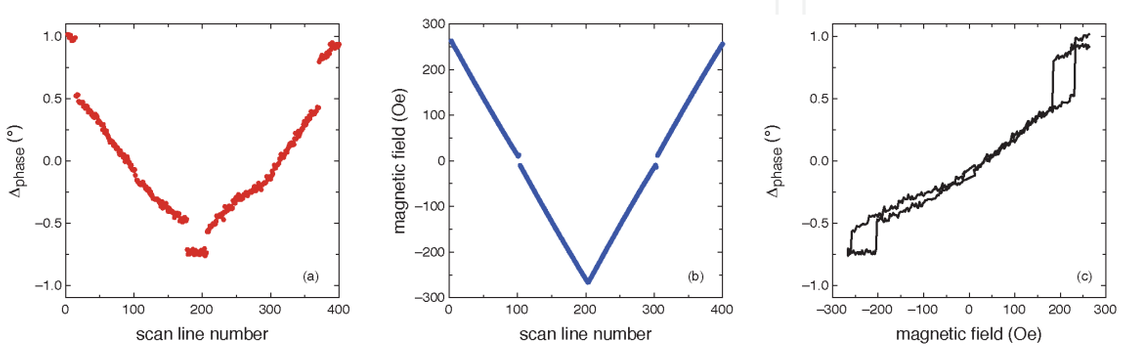

Figure 4.
*Construction of a local hysteresis loop from the data of **Figure 3**. (a) Difference of phase values as a function of the scan line number along the yellow lines of **Figure 3(b)**. (b) Applied field value as a function of scan line number, extracted from any vertical section of **Figure 3(c)**. (c) Merge of panels (a) and (b) by removing the common parameter (scan line number), resulting in the local hysteresis loop.*

2, phase channel, meaning that the magnetisation, at those field values, is less perpendicular to the square sides, i.e. less aligned to the applied magnetic field. Abrupt or peculiar features may appear, as in **Figure 4(c)**, in correspondence of specific features of the magnetisation reversal processes, for example vortex nucleation and expulsion, also putting in evidence their hysteretic behaviour.

The "dynamic scanning mode" operation of the MFM allows a great versatility, and is not limited to the field-dependent characterisations of patterned structures, such as the squares discussed so far. An example of an alternative application of the same method is shown in **Figure 5**, where a continuous thin film of $Fe_{78}Si_9B_{13}$ (thickness 230 nm) annealed at 250 °C for 1 h is investigated, through VSM and "normal scanning mode" MFM. Due to internal stresses quenched during the sputtering deposition [19], this sample is characterised by a non-negligible

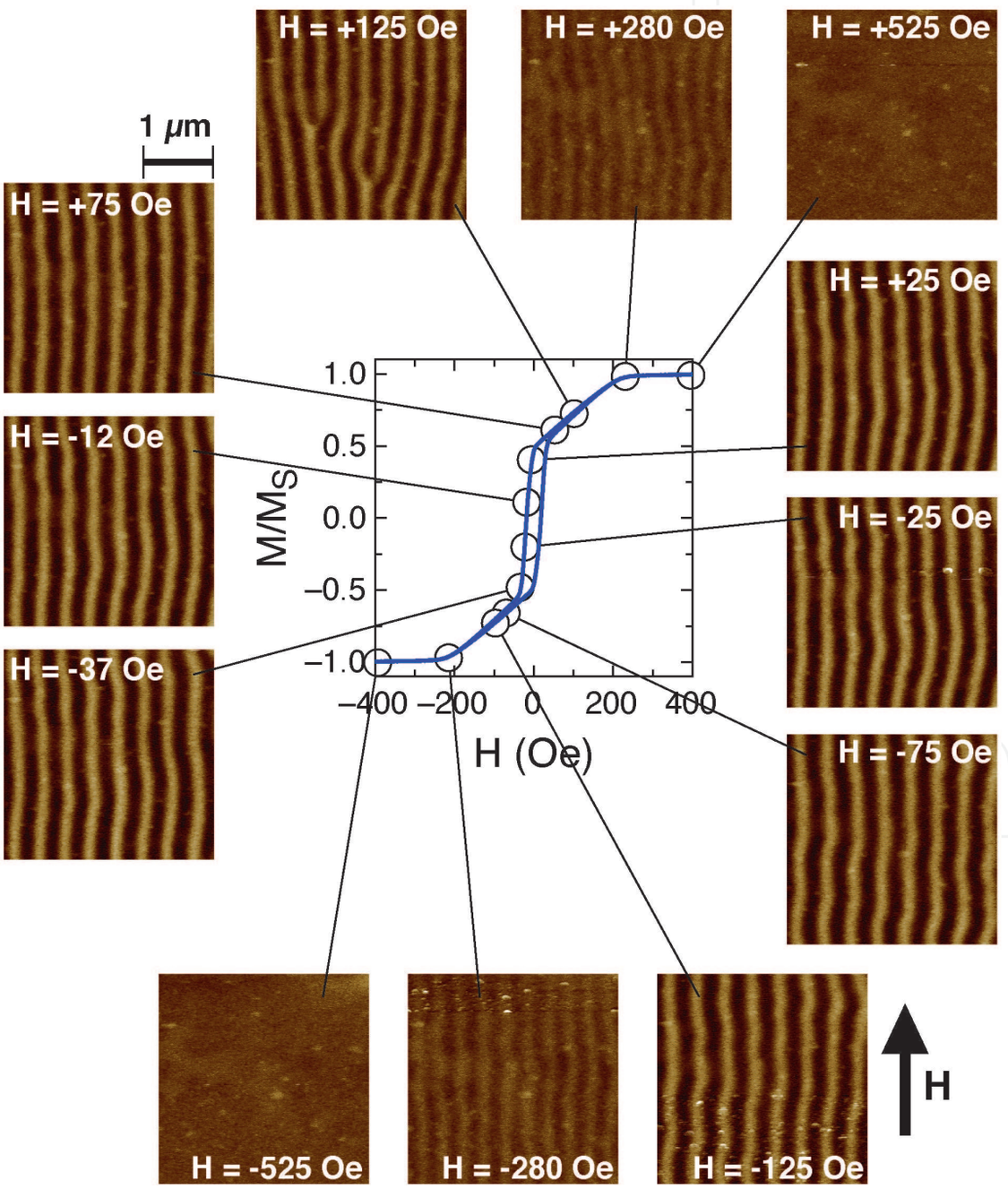

Figure 5.
Hysteresis loop and corresponding selected MFM images (acquired in "normal scanning mode") of the stripe domains of a $Fe_{78}Si_9B_{13}$ thin film (thickness 230 nm) annealed at 250 °C for 1 h. In the MFM images, the magnetic field is applied along the vertical direction. The tip is a Bruker MESP-HR.

out-of-plane magnetic anisotropy, that is responsible for the dense stripe domain configuration clearly visible in the MFM images, and for the characteristic hysteresis loop shape. In each stripe, the magnetisation is tilted with respect to the sample plane, having an in-plane component (parallel to the applied field) that gives no magnetic contrast, and an out-of-plane component, alternately up and own, that is the source of the magnetic contrast visible at the MFM. At low applied field values, where the colour contrast between the bright and dark stripes is particularly evident, the applied field (parallel to the stripes orientation) does marginally affect the magnetisation vector, by slightly rotating it toward the film plane. However, when the hysteresis loop changes slope, two effects take place at the same time, as visible at the MFM: the magnetic contrast gradually fades out, and the number of stripes visible in each MFM images changes. The gradual reduction of the magnetic contrast is due to the progressive tilt of the magnetisation vector toward the applied field direction: the out of plane component of the magnetisation reduces as the field is increased, eventually disappearing when the field is strong enough to overcome the out-of-plane anisotropy and force the magnetisation in the sample plane. The variation of the number of stripes visible in each image, instead, can be appreciated by directly counting them, and is due to bifurcation processes that can sometimes be identified in an MFM image, such as that acquired at an applied field of +125 Oe.

The "dynamic scanning mode" turns out to be particularly powerful to investigate this specific process [20]. Provided that the fast scan axis is set perpendicular to the stripes orientation, and therefore the applied field direction orthogonal to it, an image such as that shown in **Figure 6** can be obtained, detailing the evolution of the stripes domain configuration of the sample as a function of the applied field, for the same loop branch along which a few MFM images in "normal scanning mode" where discussed in **Figure 5**. The versatility of the "dynamic scanning mode" appears one more time evident: as the sample domain configuration is constituted by long, parallel stripes, the information obtained by acquiring full MFM images in "normal scanning mode" is somewhat redundant, a single profile being able to summarise a whole image. In fact, the single profile provides at the same time the magnetic contrast between the bright and dark stripes, and their number. But in "dynamic scanning mode" a single MFM image consists of the same profile acquired several hundreds of times (as compared to 12 images available in "normal scanning mode" in **Figure 5**), therefore giving with a significant magnetic field resolution the evolution of the dense stripe domain configuration. In particular, not only the magnetic contrast can be seen to gradually fade out, but the abrupt discontinuities in the stripes in **Figure 6** are a

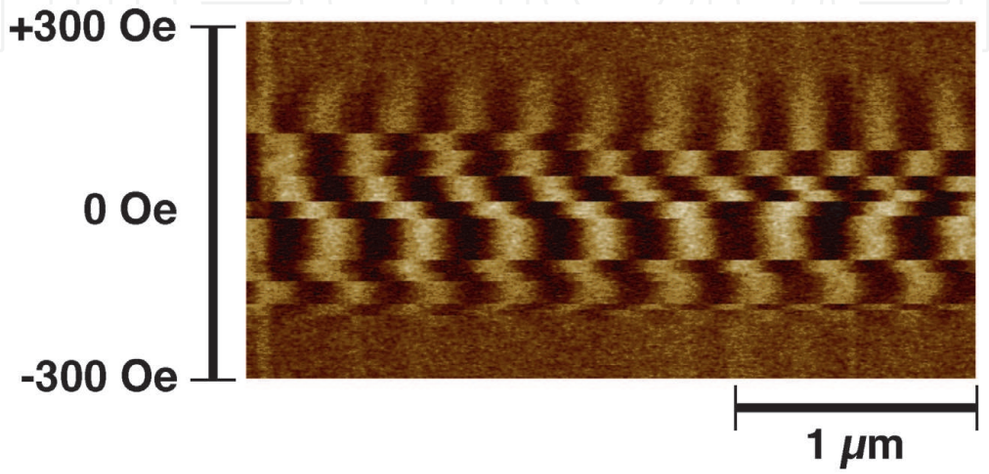

Figure 6.
MFM image acquired in "dynamic scanning mode" of the same sample shown in ***Figure 5****. The tip is a Bruker MESP-HR.*

clear indication that at those applied field values bifurcations have appeared in the vicinity of the scanned profile, giving rise to an offset of the stripes position along the profile and possibly to a variation in their number.

As it is the case for the hysteresis loops measured in "dynamic scanning mode" on the $Fe_{50}Pd_{50}$ squares, also in the case of the dense stripe domain configuration the two MFM techniques should be exploited together, along with other measurement techniques, to gain a detailed understanding of the magnetisation processes [17], paving the way to more complex investigations such as chirality control in dots [21] and rotatable anisotropy experiments [20].

4. Variations

The possibility to apply a magnetic field to the AFM, combined with the "dynamic scanning mode", actually opens new possibilities, not limited to the investigation of magnetic domains configuration evolution or to the measurement of local hysteresis loops. As an example, **Figure 7** schematically illustrates how the "dynamic scanning mode" can be exploited to measure the magnetostrictive properties of thin films [22]. In this application, the studied material is not the sample scanned by the tip, as in conventional AFM characterisations. Instead, it is the coating applied to a soft AFM cantilever (blue layer in **Figure 7**), that is brought in contact with a flat surface (green rectangle), while keeping equal to zero the field of view (0 nm scan size along both fast and slow scan axes). In practice, the AFM tip touches the flat surface and does not move while "scanning". When a magnetic field is applied, the magnetostrictive coating on the bottom side of the cantilever extends, and the cantilever bends upward (**Figure 7(b)**). This configuration, however, is out-of-equilibrium, as the AFM feedback loop will quicly react by retracting the piezo scanner (the orange block in **Figure 7**) to compensate for the apparent height variation of the sample. The adhesion forces between the tip and the flat surface ensure that the cantilever will follow the piezo scanner retracting, and will restore its initial flat configuration. The vertical retraction of the piezo scanner gives a measurement of the vertical deflection of the cantilever due to the elongation of the magnetostrictive layer on its bottom surface. In this experiment, the "dynamic scanning mode" operates exactly as discussed before, by synchronising the magnetic field changes with the EOL signal of the AFM controller. In fact, even if the scan size of the tip is equal to zero, the AFM still operates by acquiring an image where, simply, all collected data points (along each line, and for all lines) belong to the same position on the flat surface. As each line is acquired under a different

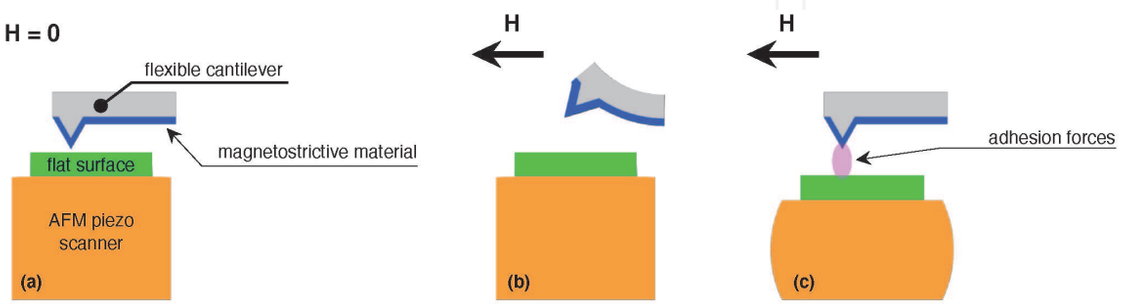

Figure 7.
Schematic representation of the operation principle of the magnetostriction measurement setup exploiting an AFM. (a) Flat cantilever in contact with a flat surface (green rectangle) with zero applied magnetic field. (b) Under an applied field H the cantilever bends upward because of the presence of a magnetostrictive material (blue layer) on its bottom. (c) The AFM feedback loop retracts the scanner (orange rectangle) to compensate for the apparent vertical displacement of the cantilever. Adhesion forces (region highlighted with a magenta shade) ensure that the cantilever follows the motion of the piezo scanner until its flat configuration is restored.

applied field, different cantilever deflection values are obtained, which can be combined to reproduce a deflection *vs.* field curve representative of the magnetostrictive response of the magnetic coating of the cantilever.

An example is provided in **Figure 8** for a $Fe_{81}Al_{19}$ coating with a thickness of 270 nm, which is compared to its hysteresis loop measured with a VSM. In **Figure 8(b)** a magnification of the region highlighted with a magenta shade shows the excellent correspondence between the peak of the deflection curve and the coercivity of the material.

The application briefly discussed in **Figures 7** and **8** provides a hint to the versatility of the AFM "dynamic scanning mode", that is in principle much more general than discussed in this chapter. In fact, the technique has only a few very general requirements:

- the material to be studied must have a property that can be investigated through an AFM (e.g. its magnetisation or its magnetostriction);
- this property must change through an externally controlled input quantity (e.g. a magnetic field);
- the externally controlled input quantity must be set fast enough to be compatible with the typical line trace times of the AFM being used; therefore, input quantities with a long inertia (e.g. a temperature) might be less convenient for these applications, whereas faster ones (e.g. electric or magnetic fields) are more appropriate;
- there must be a software or hardware arrangement enabling the control of the external input quantity triggered by the EOL signal of the AFM controller;
- there must be a way to feed the AFM controller with an analog signal proportional with the value of the externally controlled input quantity (e.g. a gaussmeter), so that its value for each line can be associated with the other channels acquired by the microscope during the "dynamic scanning".

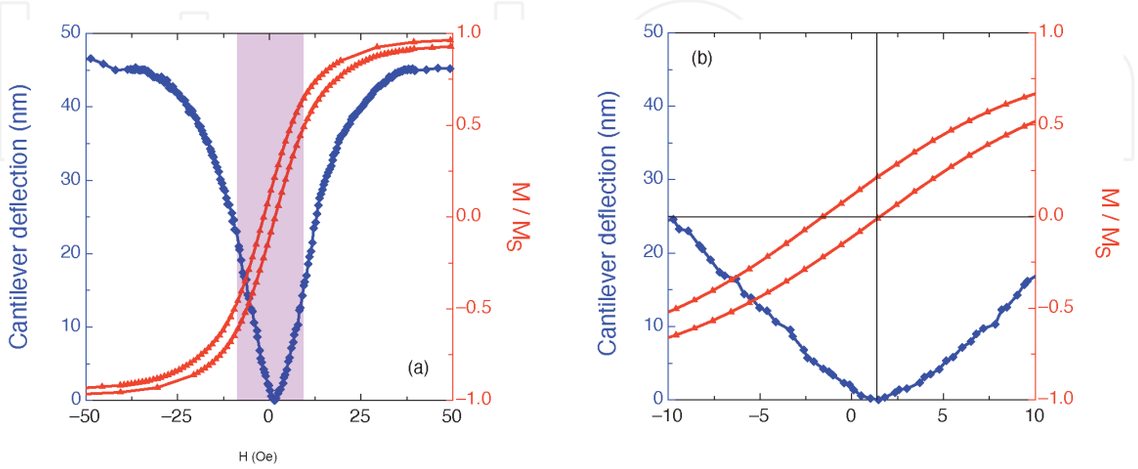

Figure 8.
(a) Cantilever deflection as a function of the applied magnetic field (blue symbols, axis and legend), compared with the magnetic hysteresis loop (red symbols, axis and legend) for a $Fe_{81}Al_{19}$ thin film with a thickness of 270 nm. (b) The same as in (a), but magnified in the magenta-shaded region. The horizontal and vertical lines mark the coincidence of coercivity with the peak of the deflection curve. The cantilevers were Nanosensors Pointprobes with a length of 445 μm, a width of 50 μm, a thickness of 2 μm, and a nominal value of elastic constant of 0.3 N/m.

These general requirements allow the design of complex and custom experiments, exploiting the versatility of an AFM, at the nanoscale, of which the study of local hysteresis loops, magnetic field evolution of domains in patterned media, and magnetostrictive response of thin films are just a few examples.

5. Conclusions

A magnetic field-dependent MFM, derived from the single-point technique, has been illustrated in its operating principles, showing a few examples of characterisations where the evolution of the magnetic domain configuration of a sample is studied as a function of the applied magnetic field. Using the same technique, local hysteresis loops have been investigated on patterned $Fe_{50}Pd_{50}$ dots, as well as dense stripe domains in $Fe_{78}Si_9B_{13}$ continuous thin films. The technique has been shown to be sufficiently general to allow significant variations, such as that for the measurement of magnetostriction on $Fe_{81}Al_{19}$ thin films. The requirements for the exploitation of the "dynamic scanning mode" of AFMs have been summarised, opening the way to the design of innovative experiments in laboratories equipped with suitable atomic force microscopes.

6. Materials and methods

$Fe_{50}Pd_{50}$ thin films with thickness of 35 nm have been prepared by rf sputtering on Si/Si-oxide substrates, and then patterned by electron beam lithography into squares with lateral sizes of 800 nm and 2 μm. The material, in its as-prepared state, has a polycrystalline fcc microstructure with a soft magnetic behaviour [23].

$Fe_{78}Si_9B_{13}$ thin films with thickness of 230 nm have been prepared by rf sputtering on Si_3N_4 substrates from targets made of amorphous ribbons. They are amorphous according to X-ray diffraction [19]. They have been annealed in furnace at 250 °C for 1 h in vacuum to partially relax the quenched-in stresses, in order to make their hysteresis loop softer [24].

$Fe_{81}Al_{19}$ thin films have been deposited on Si(100) substrates and on Si AFM cantilevers (length 445 μm, width 50 μm, thickness 2 μm, elastic constant ≈0.3 N/m) by dc magnetron sputtering at the Department of Materials Science and Metallurgy, Cambridge University, UK [22].

Acknowledgements

The Authors would like to thank Dr. Matteo Cialone and Dr. Wilhelm Hüttenes for helping with the magnetostriction measurements.

Conflict of interest

The authors declare no conflict of interest.

Abbreviations

AFM	Atomic force microscope /microscopy
EOL	End of line

MFM	Magnetic force microscope/microscopy
TTL	Transistor-to-transistor logic
VSM	Vibrating sample magnetometer/magnetometry

Author details

Marco Coïsson*, Gabriele Barrera, Federica Celegato and Paola Tiberto
INRIM, Advanced Materials and Life Sciences Division, Torino, Italy

*Address all correspondence to: m.coisson@inrim.it

References

[1] Hartmann U. High-resolution magnetic imaging based on scanning probe techniques. Journal of Magnetism and Magnetic Materials. 1996;157-158:545-549. https://doi.org/10.1016/0304-8853(95)01264-8

[2] Binning G, Quate CF, Gerber Ch. Atomic force microscope. Physical Review Letters. 1986;56:930. https://doi.org/10.1103/PhysRevLett.56.930

[3] Vock S, Wolny F, Mühl T, Kaltofen R, Schultz L, Büchner B, Hassel C, Lindner J, Neu V. Monopolelike probes for quantitative magnetic force microscopy: calibration and application. Applied Physics Letters. 2010;97:252505. https://doi.org/10.1063/1.3528340

[4] Hug HJ, Stiefel B, van Schendel PJA, Moser A, Hofer R, Martin S, Güntherodt H-J. Quantitative magnetic force microscopy on perpendicularly magnetised samples. Journal of Applied Physics. 1998;83:5609. https://doi.org/10.1063/1.367412

[5] Zhu X, Grütter P, Metlushko V, Ilic B. Magnetization reversal and configurational anisotropy of dense permalloy dot arrays. Applied Physics Letters. 2002;80:4789. https://doi.org/10.1063/1.1489720

[6] Yang JKW, Chen Y, Huang T, Duan H, Thiyagarajah N, Hui HK, Leong SH, Ng V. Fabrication and characterisation of bit-patterned media beyond 1.5 Tbit/in^2. Nanotechnology. 2011;22:385301. https://10.1088/0957-4484/22/38/385301

[7] Piramanayagam SN, Ranjbar M, Sbiaa R, Tavakkoli AKG, Chong TC, Characterisation of high-density bit-patterned media using ultra-high resolution magnetic force microscopy. Physica Status Solidi Rapid Research Letters. 2012;6(3):141-143. https://doi.org/10.1002/pssr.201105537

[8] Imre A, Csaba G, Ji L, Orlov A, Bernstein GH, Porod W. Majority logic gate for magnetic quantum-dot cellular automata. Science. 2006;311(5768):205-208. https://doi.org/10.1126/science.1120506

[9] Li H, Qi X, Wu J, Zeng Z, Wei J, Zhang H. Investigation of MoS_2 and graphene nanosheets by magnetic force microscopy. ACS Nano. 2013;7(3):2842-2849. https://doi.org/10.1021/nn400443u

[10] Israel C, de Lozanne A. High-field magnetic force microscopy as susceptibility imaging. Applied Physics Letters. 2006;89:032502. https://doi.org/10.1063/1.2221916

[11] Sorop TG, Untiedt C, Luis F, Kröll M, Raşa M, de Jongh LJ. Magnetisation reversal of ferromagnetic nanowires studied by magnetic force microscopy. Physical Review B. 2003;67:014402. https://doi.org/10.1103/PhysRevB.67.014402

[12] Zhu X, Grütter P, Metlushko V, Hao Y, Castaño FJ, Ross CA, Ilic B, Smith HI. Construction of hysteresis loops of single domain elements and coupled permalloy ring arrays by magnetic force microscopy. Journal of Applied Physics. 2003;93:8540. https://doi.org/10.1063/1.1540129

[13] Zhu X, Grütter P. Imaging, manipulation and spectroscopic measurements of nanomagnets by magnetic force microscopy. MRS Bulletin. 2004;29(7):457-462. https://doi.org/10.1557/mrs2004.139

[14] Rastei MV, Meckenstock R, Bucher JP. Nanoscale hysteresis loop of individual Co dots by field-dependent magnetic force microscopy. Applied

Physics Letters. 2005;87:222505. https://doi.org/10.1063/1.2138349

[15] Jaafar M, Serrano-Ramón L, Iglesias-Freire O, Fernández-Pacheco A, Ibarra MR, De Teresa JM, Asenjo A. Hysteresis loops of individual Co nanostripes measured by magnetic force microscopy. Nanoscale Research Letters. 2011;6:407. https://doi.org/10.1186/1556-276X-6-407

[16] Grütter P, Jung Th, Heinzelmann H, Wadas A, Meyer E, Hidber H-R, Güntherodt H-J. 10-nm resolution by magnetic force microscopy on FeNdB. Journal of Applied Physics. 1990;67:1437. https://doi.org/10.1063/1.345675

[17] Coïsson M, Barrera G, Celegato F, Enrico E, Manzin A, Olivetti ES, Tiberto P, Vinai F. Local field loop measurements by magnetic force microscopy. Journal of Physics D: Applied Physics. 2014;47:325003. https://doi.org/10.1088/0022-3727/47/32/325003

[18] Coïsson M, Barrera G, Celegato F, Tiberto P. Development and calibration of a MFM-based system for local hysteresis loops measurements. Journal of Physics: Conference Series. 2016;755:012002. https://doi.org/10.1088/1742-6596/755/1/012002

[19] Coïsson M, Celegato F, Olivetti E, Tiberto P, Vinai F, Baricco M. Stripe domains and spin reorientation transition in $Fe_{78}B_{13}Si_9$ thin films produced by rf sputtering. Journal of Applied Physics. 2008;104:033902. https://doi.org/10.1063/1.2960454

[20] Coïsson M, Barrera G, Celegato F, Tiberto P. Rotatable magnetic anisotropy in $Fe_{78}Si_9B_{13}$ thin films displaying stripe domains. Applied Surface Science. 2019;476:402-411. https://doi.org/10.1016/j.apsusc.2019.01.126

[21] Coïsson M, Barrera G, Celegato F, Manzin A, Vinai F, Tiberto P. Magnetic vortex chirality determination via local hysteresis loops measurements with magnetic force microscopy. Scientific Reports. 2016;6:29904. https://doi.org/10.1038/srep29904

[22] Coïsson M, Hüttenes W, Cialone M, Barrera G, Celegato F, Rizzi P, Barber ZH, Tiberto P. Measurement of thin films magnetostriction using field-dependent atomic force microscopy. Applied Surface Science. 2020;525:146514. https://doi.org/10.1016/j.apsusc.2020.146514

[23] Tiberto P, Celegato F, Barrera G, Coisson M, Vinai F, Rizzi P. Magnetization reversal and microstructure in polycrystalline $Fe_{50}Pd_{50}$ dot arrays by self assembling of polystyrene nanospheres. Science and Technology of Advanced Materials. 2016;17(1):462-472. https://doi.org/10.1080/14686996.2016.1201414

[24] Tiberto P, Celegato F, Coïsson M, Vinai F. Spin reorientation transition in amorphous FeBSi thin films submitted to thermal treatments. IEEE Transactions on Magnetics. 2008;44(11):3921-3924. https://doi.org/10.1109/TMAG.2008.2002255